Support Information

Facile Synthesis of Single-atom Electrocatalysts with Tailored Carbon Architectures via a Polyelectrolyte Brush-templated-growth Approach

Zhinan Fu[1, 2]†, Lizhen Wang[1]†, Weijun Zhang[1], Xuan Tang[1], Wenxin Xia[1], Jinxia Li[1], Kuanwen Wang[3], Lihui Zhou[1], Xuhong Guo[2], Sheng Dai[1*]*

1 Key Laboratory for Advanced Materials and Joint International Research Laboratory of Precision Chemistry and Molecular Engineering, Feringa Nobel Prize Scientist Joint Research Centre, School of Chemistry and Molecular Engineering, East China University of Science & Technology, Shanghai 200237, China

2 State Key Laboratory of Chemical Engineering, East China University of Science and Technology, 200237 Shanghai, P.R. China

3 Institute of Materials Science and Engineering, National Central University, Taoyuan 320, Taiwan

†These authors contributed equally to this work.

Experimental Section

Materials

Acetone, pyridine, styrene, acrylic acid (AA) and potassium persulfate (KPS) were purchased from Sinopharm Chemical Reagent Co., Ltd. Pyridine, styrene, and AA were purified by reduced pressure distillation and store at 2-6 °C. Ethanol, methanol, KOH, $Zn(NO_3)_2 \cdot 6H_2O$ were purchased from Sinopharm Chemical Reagent Co., Ltd. Methacryloyl chloride, $FeCl_2 \cdot 4H_2O$, $CoCl_2 \cdot 6H_2O$, and $PdCl_2$ were purchased from Shanghai Macklin Biochemical Co., Ltd. 2-methylimidazole and sodium dodecyl sulfonate (SDS) were purchased from Aladdin. 5 % Nafion and 2-Hydroxy-4'-(2-hydroxyethoxy)-2-methylpropiophenone (HMP) were bought from Sigma-Aldrich. $CuCl_2 \cdot 2H_2O$ was purchased from Meryer (Shanghai) Chemical Technology Co., Ltd. All chemicals were of analytical grade. Distilled ultrapure water was used for all solution preparation and cleaning products.

Preparation of HMEM

HMEM was synthesized according to our previous work [X. Guo, A. Weiss, M. Ballauff, Macromolecules 1999, 32, 6043-6046]. Briefly, HMP (30 g) and acetone solution (150 mL) were added into a three-necked round-bottom flask, and then stirred until the HMP was completely dissolved. Then, pyridine (10 mL) was added into this solution. The methylacryloyl chloride (13.6 g) dissolved in acetone solution (50 mL) was injected into the flask at a controlled dropping rate of 6-7 s per drop in the dark and stirred for 30 min in an ice bath, and for another 12 h at room temperature. The highly purified HMEM was obtained through chromatography.

Preparation of PS nanosphere.

Polystyrene colloidal nanosphere was synthesized by emulsion polymerization method. First, SDS (0.4 g), KPS (0.6 g), styrene (10 g) and deionized water (250 g) were added into a four-necked round-bottom flask. The mixed solution was stirred for 15 min at 300 rpm, and then the polymerization was conducted at 80 °C under nitrogen atmosphere. After 1 h, the reaction temperature was cooled to 70 °C. Then, the

homemade photoinitiator HMEM (1.0 g) dissolved in acetone (8.0 g) was injected into the system at a constant dropping rate of 6-7 s per drop. Then, the reaction was continued for 1.5 h in the dark to obtain the PS nanosphere with the attached photoinitiator HMEM. The obtained product was purified by dialyzing against deionized water in the dark until the conductivity remained constant.

Preparation of PAA-SPB

The PAA-SPB with different length of PAA chains were synthesized by photo-emulsion polymerization method. A given amount of AA monomers were added into the corresponding mass of PS core with photoinitiator HMEM and the mixture was transferred into a homemade photoreactor. The reaction was carried out under UV radiation and nitrogen atmosphere for 2 h. Afterwards, the prepared three PAA-SPB with PAA chains of short, medium and long length were purified by ultrafiltration until the conductivity remained constant.

Preparation of *s/m/l*-Fe-HNC

The PAA$_{S/M/L}$-SPB (3.0 g) was dispersed in methanol (21.0 g) and stirred for 20 min. Then, $Zn(NO_3)_2 \cdot 6H_2O$ (210.5 mg) and $FeCl_2 \cdot 4H_2O$ (1.8 mg) were dispersed in methanol (3.6 ml). Slowly dropped the methanol solution of Fe^{2+} and Zn^{2+} into PAA$_{S/M/L}$-SPB methanol solution and stirred for 30 min, then added into a methanol solution containing 1.2 g of 2-methylimidazole under vigorously stirring. Nitrogen atmosphere was maintained in the reactor during the whole process. After stirring for 7 h, the precipitates were collected by centrifugation at 8000 rpm, washed three times with methanol, and dried at room temperature in vacuum overnight. The collected samples were pyrolyzed in a tube furnace at 900 °C for 3 h under flowing nitrogen. The as-prepared samples were denoted as *s/m/l*-Fe-HNC and used for further characterization without any post-treatments. For Co, Cu, and Pd-based single-atom catalysts, $CoCl_2 \cdot 6H_2O$, $CuCl_2 \cdot 2H_2O$, and $PdCl_2$ were used as the metal precursors, respectively.

Preparation of N-C

The PAA$_S$-SPB (3.0 g) was dispersed in methanol (21.0 g) and stirred for 20 min. Then, Zn(NO$_3$)$_2$·6H$_2$O (210.5 mg) was dispersed in methanol (3.6 ml). Slowly dropped the methanol solution of Zn^{2+} into the PAA$_S$-SPB methanol solution and stirred for 30 min and then added into a methanol solution containing 1.2 g of 2-methylimidazole under vigorously stirring. Nitrogen atmosphere was maintained in the reactor during the whole process. After stirring for 7 h, the precipitates were collected by centrifugation at 8000 rpm, washed three times with methanol, and dried at room temperature in vacuum overnight. The collected samples were pyrolyzed in a tube furnace at 900 °C for 3 h under flowing nitrogen.

Preparation of Fe-N-C

Zn(NO$_3$)$_2$·6H$_2$O (210.5 mg) and FeCl$_2$·4H$_2$O (1.8 mg) were dispersed in methanol (24 ml). stirred for 30 min and then added into a methanol solution containing 1.2 g of 2-methylimidazole under vigorously stirring. Nitrogen atmosphere was maintained in the reactor during the whole process. After stirring for 7 h, the precipitates were collected by centrifugation at 8000 rpm, washed three times with methanol, and dried at room temperature in vacuum overnight. The collected samples were pyrolyzed in a tube furnace at 900 °C for 3 h under flowing nitrogen.

Materials characterization

Scanning electron microscopy (Helios G4 UC, Thermo Scientific, US), transmission electron microscopy (Talos F200X, Thermo Scientific, US), and aberration-corrected transmission electron microscope (Themis Z, Thermo Scientific, US) were used to characterize the morphology and the microstructure. The powder X-ray diffraction (D/max 2550, Rigaku, Japan) from 5 to 75 degree was determined by using Cu Kα radiation at 40 kV and 100 mA. Nitrogen adsorption-desorption isotherms were measured on a Micromeritics ASAP-2020 instrument, where the Brunauer-Emmett-Teller (BET) and density functional theory (DFT) methods were used to characterize the specific surface areas and pore size distribution. The XPS data was conducted with an X-ray photoelectron spectrometer (ESCALAB 250Xi,

Thermo Scientific, US). Fe content was detected with ICP-AES (Agilent 725ES, US).

Electrochemical characterization

All of the electrochemical analyses were performed at room temperature using rotating disk electrode (RDE) and rotating ring-disk electrode (RRDE) techniques on a Parstat 4000 (Princeton Applied Research) electrochemical workstation combined with a conventional three-electrode cell, that is, the catalyst modified GCE as the working electrode, an Ag/AgCl KCl (3 M) electrode as the reference electrode, and a Pt wire as the counter electrode. All potentials in this study were converted versus reversible hydrogen electrode (RHE) according to: *E(vs. RHE) = E(vs. Ag/AgCl)+$E^0_{Ag/AgCl}$ +0.0592 pH*. The homogeneous inks were prepared as follows: 5 mg catalyst and 30 µL of 5 wt% Nafion were dispersed in 1 mL mixed solution of isopropanol and H_2O (isopropanol 333 µL,H_2O 666 µL). Then 13 µL of the catalyst ink was loaded onto the surface of RDE and dried at room temperature.

The ORR performances of Fe-HNC electrocatalysts were measured by cyclic voltammetry (CV) and linear sweep voltammetry (LSV). By bubbling O_2 or N_2 for 30 min, the electrolyte was saturated with oxygen or nitrogen before the measurements. CV curves were recorded in a N_2- and O_2- saturated 0.1 M KOH solution between 0 and 1.2 V (vs RHE) with a scan rate of 50 mV s^{-1}, and LSV measurements were conducted in an O_2- saturated 0.1 M KOH solution from 1.15 to 0.2 V (vs RHE) at a scan rate of 10 mV s^{-1} and a rotation rate of 1600 rpm. Kinetic current density were determined by Koutecky-Levich equation:

$1/J=1/J_D+1/J_K=1/B\omega^{1/2}+1/J_K$

where *J* is the current density, J_K and J_L are the measured kinetic and diffusion-limited current densities, respectively, ω is the angular velocity.

The calculation of electrochemically active surface area (ECSA) is based on the measured double layer capacitance of samples on glassy carbon RDE in 0.1 M KOH.

A potential range of 0.00 to 0.10 V vs. Ag/AgCl was chosen for the capacitance measurements where no faradic processes were observed at the scan rates of 1, 2, 4, 6, 8 and 10 mV s^{-1}, respectively. The relation between i_c, the scan rate (v) and the double layer capacitance (C_{DL}) was given in eq 1.

$i_c=v \times C_{DL}$ (1)

Therefore, the slope of i_c, as a function of v, will give a straight line with the slope equal to C_{DL}. For the estimation of ECSA, a specific capacitance (C_s) value C_s =0.040 mF cm^{-2} in 0.1 M KOH . As a result, the ECAS can be calculated according to eq 2.

ECSA= C_{DL}/ C_s
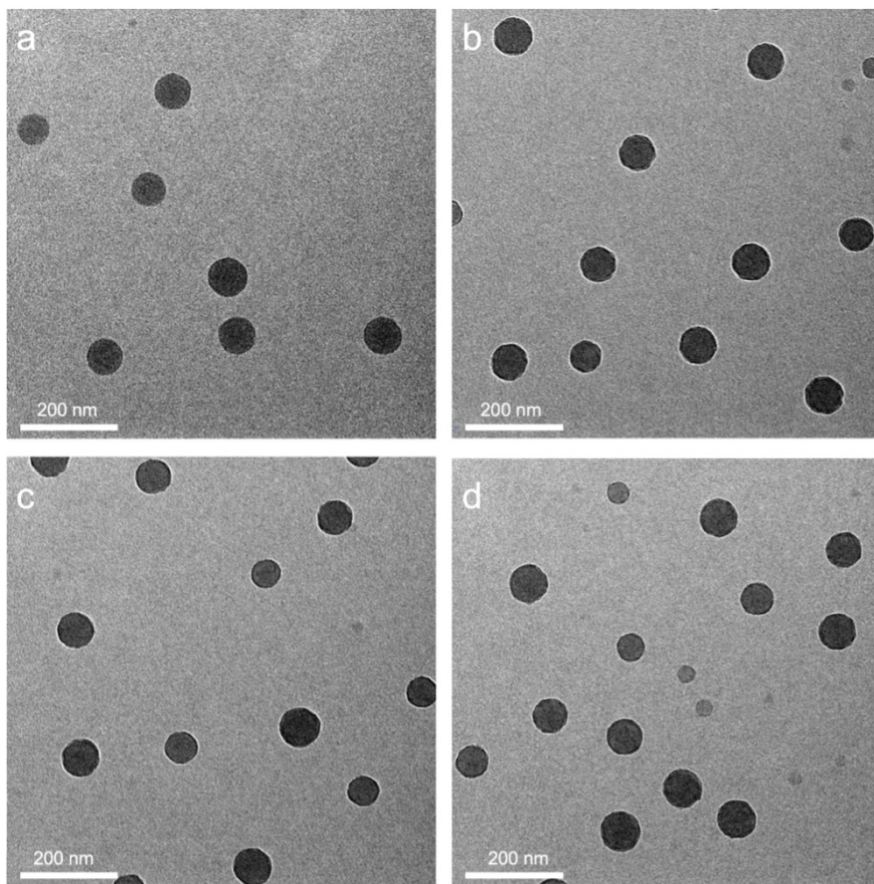
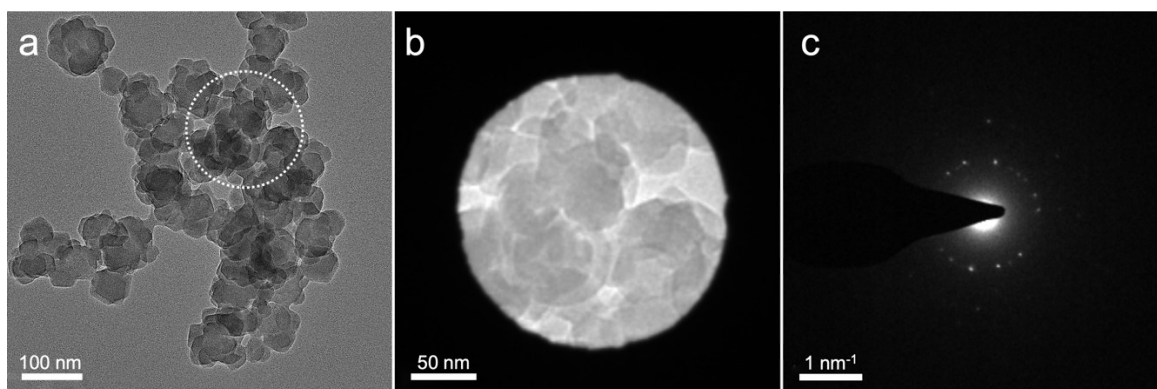**Figure S1.** TEM images of (a) PS, (b) PAA$_S$-SPB, (c) PAA$_M$-SPB, and (d) PAA$_L$-SPB.

Figure S2. TEM characterization of the as-prepared Fe-ZIF@PAA$_S$-SPB. (a-b) TEM image and the selected region of Fe-ZIF@PAA$_S$-SPB. (c) Electron diffraction of the selected region in (b).
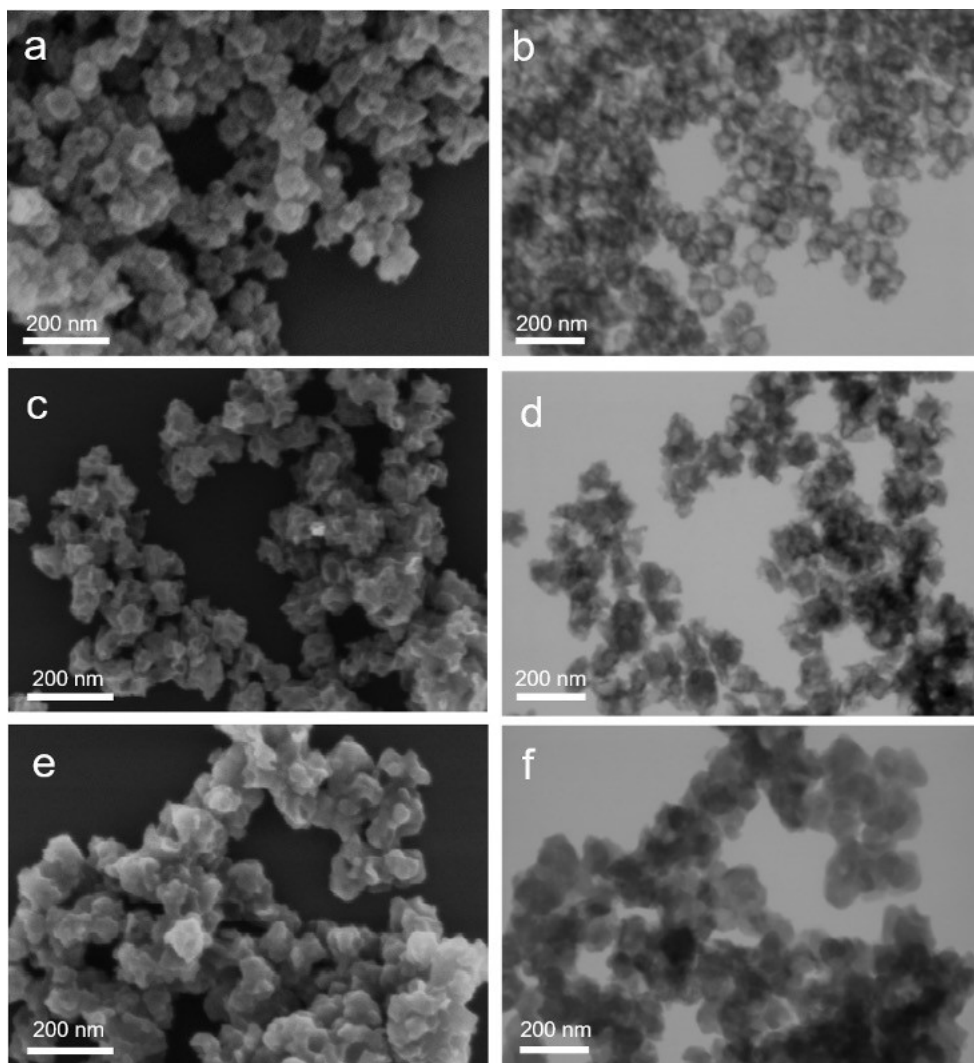
Figure S3. SEM and 30 kV STEM-based BF-STEM images of (a, b) *s*-Fe-HNC, (c, d) *m*-Fe-HNC and (e, f) *l*-Fe-HNC.
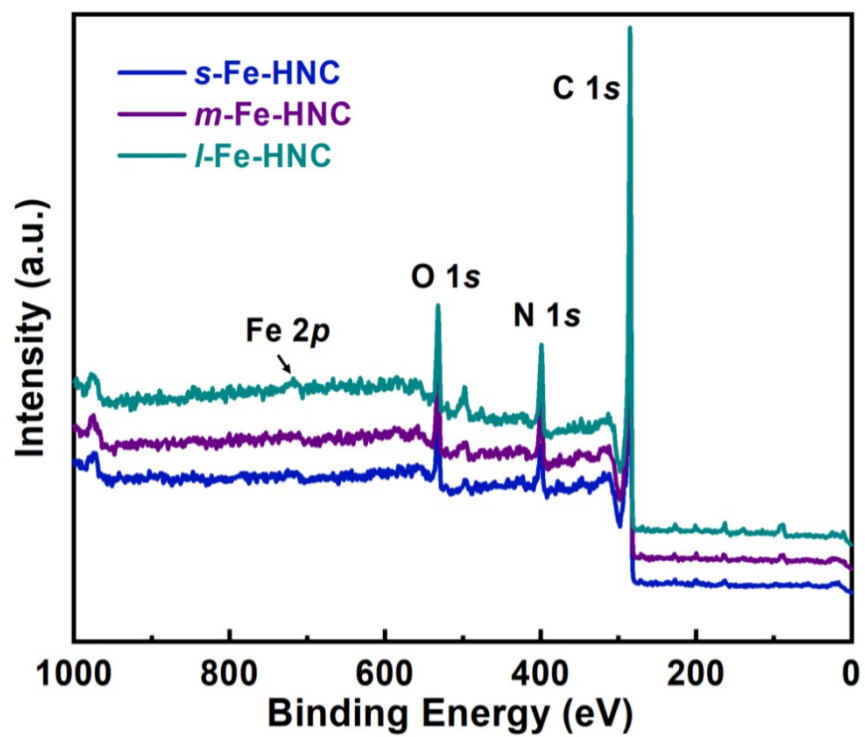
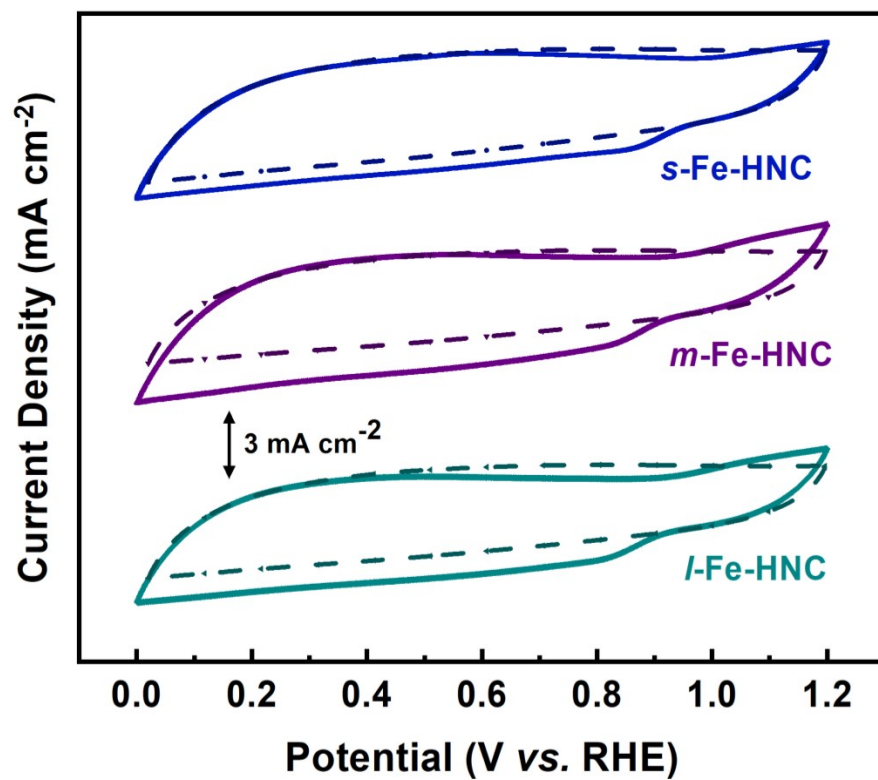**Figure S4.** XPS survey spectra of *s*-Fe-HNC, *m*-Fe-HNC and *l*-Fe-HNC.

Figure S5. CV curves of *s*-Fe-HNC, *m*-Fe-HNC and *l*-Fe-HNC in O_2-saturated (solid line) or N_2-saturated (dashed line) in 0.1 M KOH at a sweep rate of 50 mVs^{-1}.
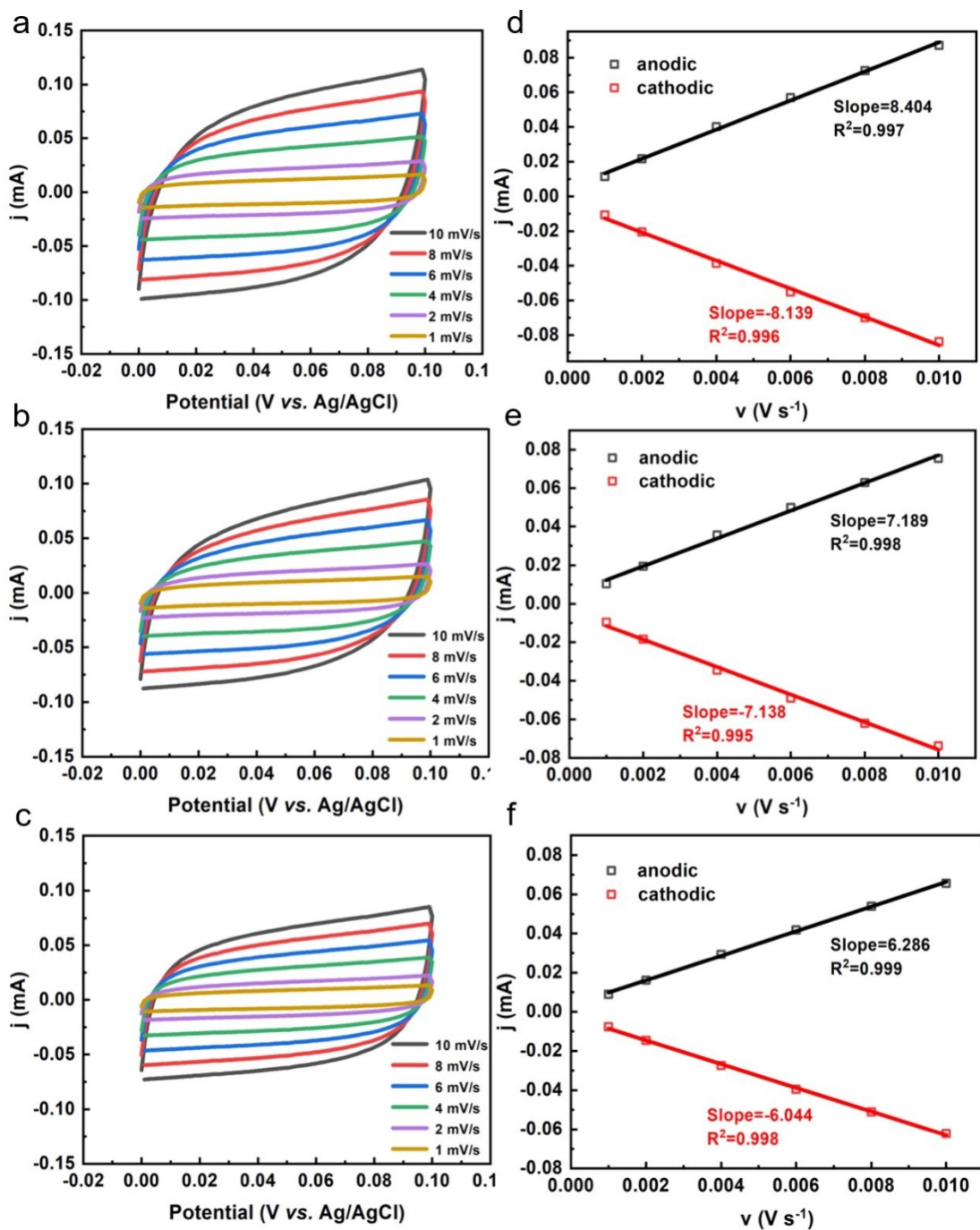
Figure S6. CVs of (a) *s*-Fe-HNC, (b) *m*-Fe-HNC and (c) *l*-Fe-HNC were measured in a non-Faradaic region of the voltammogram at different scan rates of 1, 2, 4, 6, 8 and 10 mV s^{-1} in 0.1 M KOH. The cathodic (red open circle) and anodic (black open square) charging currents measured at 0 V vs. Ag/AgCl plotted as a function of scan rate. The determined double-layer capacitance of (d) *s*-Fe-HNC, (e) *m*-Fe-HNC and (f) *l*-Fe-HNC were taken as the average of the absolute value of the slope of the linear fits to the data.
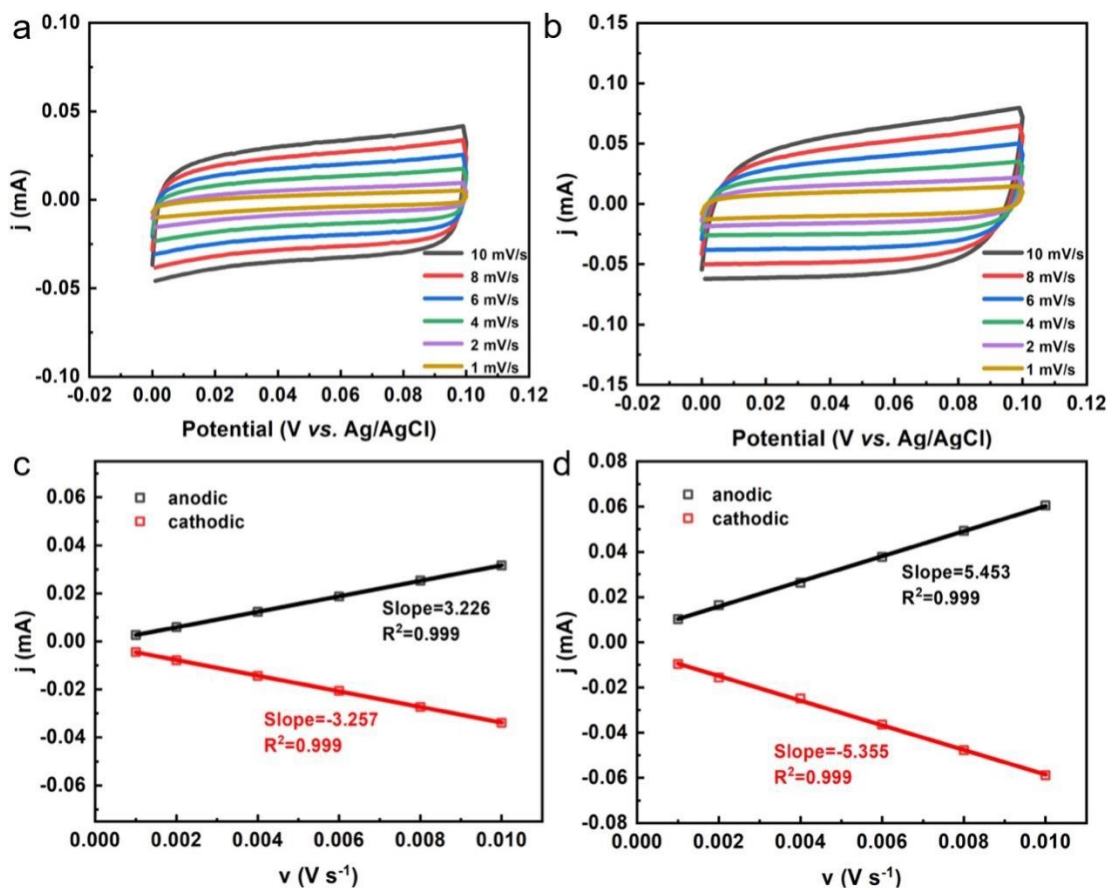
Figure S7. CVs of (a) commercial Pt/C and (b) Fe-N-C were measured in a non-Faradaic region of the voltammogram at different scan rates of 1, 2, 4, 6, 8 and 10 mV s^{-1} in 0.1 M KOH. The cathodic (red open circle) and anodic (black open square) charging currents measured at 0 V vs. Ag/AgCl plotted as a function of scan rate. The determined double-layer capacitance of (c) commercial Pt/C and (d) Fe-N-C were taken as the average of the absolute value of the slope of the linear fits to the data.
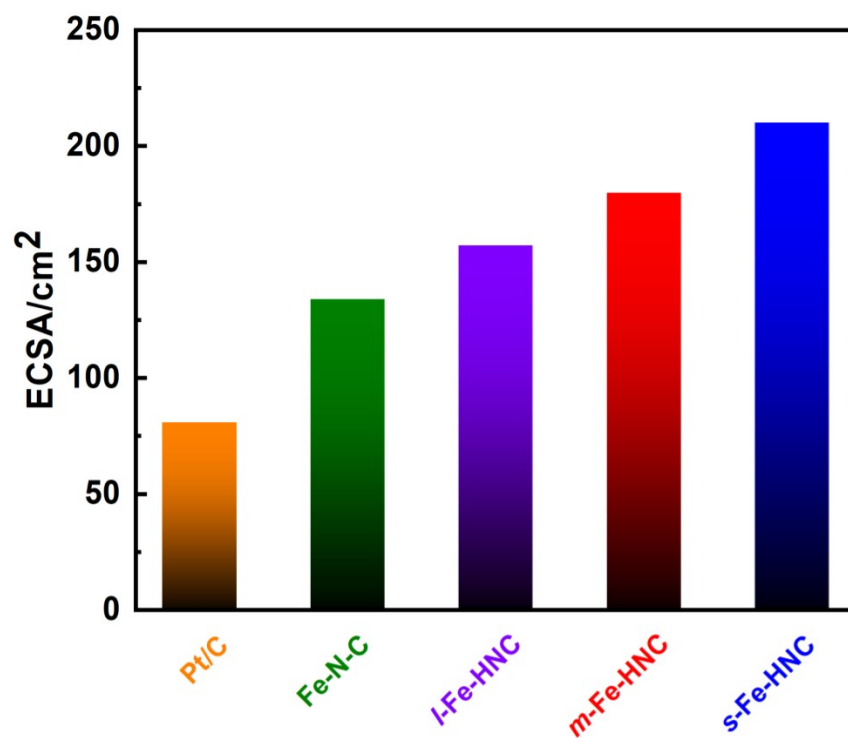
Figure S8. Electrochemical active surface area of *s*-Fe-HNC, *m*-Fe-HNC, *l*-Fe-HNC, Fe-N-C, and commercial Pt/C.
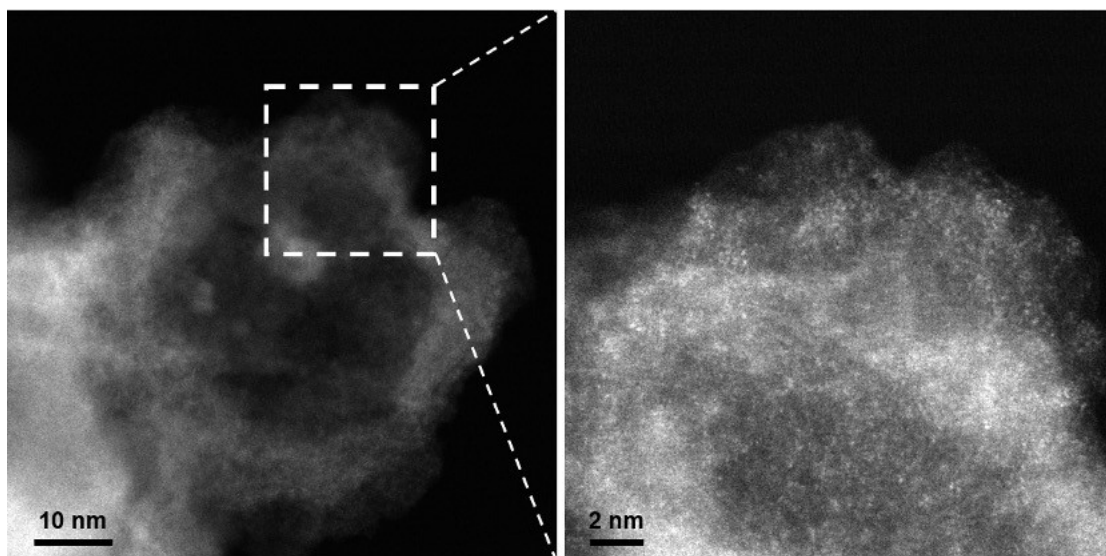
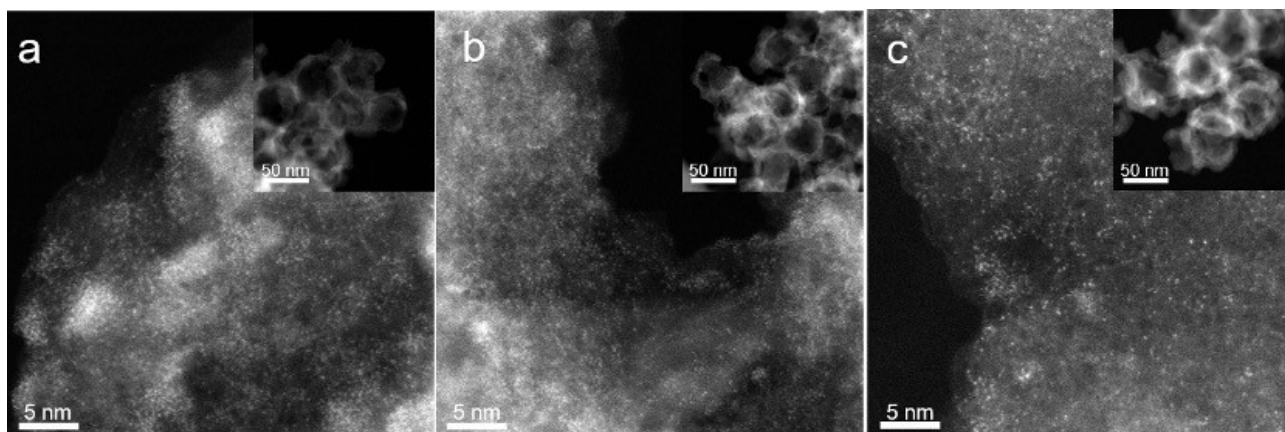**Figure S9.** Atomic-resolution HAADF-STEM images showing *s*-Fe-HNC after the stability test.

Figure S10. Atomic-resolution HAADF-STEM images of (a) *s*-Co-HNC, (b) *s*-Cu-HNC and (c) *s*-Pd-HNC.

Table S1. Fe contents of *s*-Fe-HNC, *m*-Fe-HNC and *l*-Fe-HNC measured by XPS, and relative contents of different Fe and N species in samples.

Sample	Fe at%	Fe⁰ %	Feᴵᴵ %	Feᴵᴵᴵ %	Fe-N %	Pyridinic N %	Pyrrodic N %	Graphitic N %	Oxide N %
s-Fe-HNC	0.50	0.7	79.1	20.2	30.0	16.5	19.8	24.8	8.9
m-Fe-HNC	0.56	0.5	79.2	20.3	26.5	14.6	20.1	26.0	12.8
l-Fe-HNC	0.49	0.5	79.3	20.2	24.3	15.4	17.6	28.7	14.0

Table S2. C, N, O and Fe contents of *s*/*m*/*l*-Fe-HNC measured by XPS and ICP, respectively.

Sample	C (wt%)	N (wt%)	O (wt%)	Fe (wt%)
s-Fe-HNC	80.7	10.9	7.9	1.3
m-Fe-HNC	82.9	9.0	7.6	1.2
l-Fe-HNC	82.1	8.2	9.1	1.3

Table S3. Structural parameters of *s/m/l*-Fe-HNC extracted from the Fe K-edge EXAFS fitting data.

Sample	N_{Fe-N}	$R_{Fe-N}(\text{Å})$	$\sigma^2(\text{Å}^2)$	$\Delta E_0(eV)$	R_{factor}
s-Fe-HNC	4.5 ± 0.6	1.993 ± 0.014	0.0097 ± 0.0011	-6.2 ± 1.3	0.0180
m-Fe-HNC	4.7 ± 0.7	1.995 ± 0.015	0.0085 ± 0.0018	-4.9 ± 1.9	0.0193
l-Fe-HNC	4.6 ± 0.6	2.017 ± 0.012	0.0073 ± 0.0021	-6.5 ± 1.6	0.0148

Table S4. Comparison of the electrocatalytic ORR activity of *s*-Fe-HNC with other representative Fe single-atom electrocatalysts with ZIF-8 as precursor recently reported in the literatures.

Catalyst	Electrolyte	E1/2 (V vs. RHE)	Reference
s-Fe-HNC	0.1 MKOH	0.90	This work
Fe-N/C-1/30	0.1 M KOH	0.89	Nano Energy, 2018, 52, 29-37
3DOM Fe-N-C-900	0.1 M KOH	0.87	Nano Energy 2020, 71, 104547
Fe@MNC-1	0.1 M KOH	0.88	ACS Appl. Mater. Interfaces 2019, 11, 25976-25985
Fe-ISAs/H-CN	0.1 M KOH	0.87	J. Mater. Chem. A, 2021, 9, 22095-22101
Fe-NC-155	0.1 M KOH	0.85	J. Mater. Chem. A, 2019, 7, 16508-16515
C-FeZIF-4.44-950	0.1 M KOH	0.86	Adv. Energy Mater.2019, 9, 1802856
C-FeHZ8@g-C_3N_4-950	0.1 M KOH	0.84	J. Mater. Chem. A, 2019, 7, 5020-5030

Table S5. Comparison of the electrocatalytic ORR activity of *s*-Fe-HNC with other representative Fe single-atom electrocatalysts recently reported in the literatures.

Catalyst	Electrolyte	E1/2 (V vs. RHE)	Reference
s-Fe-HNC	0.1 M KOH	0.90	This work
SA-Fe-HPC	0.1 M KOH	0.89	Angew. Chem. Int. Ed. 2018, 57, 9038-9043
Fe/N-MGN	0.1 M KOH	0.86	Nano Res. 2020, 13(3): 752-758
Fe-N/C-700	0.1 M KOH	0.86	Nanoscale 2018, 10, 16145-16152
Fe SA/NPCs	0.1 M KOH	0.83	Applied Catalysis B: Environmental 2020, 278, 119270
Fe SAC@G-110	0.1 M KOH	0.89	ChemSusChem 2021, 14, 866-875
NR-CNT@FeN-PC	0.1 M KOH	0.88	Nanotechnology 2021, 32(30), 305402
Fe-NCCS	0.1 M KOH	0.82	ACS Appl. Energy Mater. 2018, 1, 4982-4990